Desalination and Water Treatment
www.deswater.com

doi: 10.5004/dwt.2020.25151

192 (2020) 11–18
July

Effect of vibration on fouling propensity of hollow fiber membranes in microfiltration and membrane distillation

Youngkyu Park, Yongjun Choi, Jihyeok Choi, Jaehyun Ju, Bomin Kim, Sangho Lee*

School of Civil and Environmental Engineering, Kookmin University, 77 Jeongneung-ro, Seoungbuk-gu, Seoul 02707, Korea, Tel. +82-2-910-4529; Fax: +82-2-910-4939; email: sanghlee@kookmin.ac.kr (S. Lee)

Received 1 July 2019; Accepted 18 November 2019

ABSTRACT

Hollow fiber microporous membranes have been widely used in microfiltration (MF) for water and wastewater treatment as a pressure-driven separation process. Among them, hydrophobic membranes have been also considered in membrane distillation (MD) for seawater desalination as a thermally-driven separation process. In both cases, membrane fouling is a major bottleneck limiting their widespread applications. This study focused on the control of membrane fouling in MF and MD processes by directly vibrating the modules. Experiments were carried out using a laboratory-scale setup in both MF and MD. Synthetic feed water containing NaCl of 35,000 mg/L and $CaSO_4$ of 2,000 mg/L was used for fouling tests. Factors affecting flux were examined, including vibration, operation type. The frequency of vibration feed was adjusted from 100 to 200 Hz. Results showed that the effect of the vibration was more important in the MD process than in the MF process. In MD, the vibration was more effective in the inside-out operation mode than in the outside-in operation mode. The blocking of the membrane surface by the foulants occurs less severely with the vibration than without the vibration.

Keywords: Vibration; Fouling; Hollow fiber membrane; Microfiltration; Direct contact membrane distillation; Blocking

1. Introduction

Although hollow fiber membranes have been applied in various membrane processes, fouling is an inherent problem and should be properly resolved prior to the practical application. Membrane fouling can be controlled by several approaches, which include pretreatment of the feed solution, modification of membrane properties, and hydraulic or chemical cleaning [1]. The hydrodynamic shear stresses on the membrane surface is one of the most effective techniques for retarding fouling [2,3]. Hydrodynamic shear stresses can be generated on the membrane surface by moving either the fluid next to the membrane or the membrane surface itself. The aeration has been commonly adopted in membranes for industry applications. In addition to inducing wall shear stresses on the membrane surface, aeration also disrupts the concentration polarization layer around the hollow fibers. However, the shear stresses induced by aeration are relatively weak and the flux improvement is ineffective by increasing in the air flow rate [4–6].

Vibrating the membrane module can also induce dynamic shear stresses on the membrane surfaces for fouling mitigation. It was found that the operating power consumption with vibration is significantly less than aeration for a similar fouling rate, which can be due to the fact that only the boundary fluid layers around the fibers are mobilized

* Corresponding author.

and thus the energy dissipation is much reduced [7]. The concept modules based on the vibration have been developed in the forms of rotating disks [8], rotating membranes [9], vibrating flat membranes [10], and vibrating hollow fibers [11].

The vibration of the membrane is not a novel concept for pressure-driven membrane processes such as microfiltration (MF). However, it is a relatively new approach for membrane distillation (MD), which has drawn attention as an emerging technology for seawater desalination and water treatment [12–15]. There are many advantages in MD, including low operating energy, no pressure requirement, high rejection for ions, the ability to treat feed water containing high salinity, and a good feasibility [16–20]. There are two possible module geometries for membrane distillation. One of them is the flat sheet and the other is the hollow fiber. Since the hollow fiber module has high packing density and affordable, it is more suitable for large-scale applications [21–24]. In hollow fiber MD modules, there are several design factors influencing the process efficiency and one of them is the selection of flow direction. Unlike flat sheet MD modules, hollow fiber MD modules may be operated either inside-out or outside-in modes [25].

Thus, this study focused on the effect of vibration on the fouling propensity of hollow fiber membranes in MF and MD processes. Moreover, the vibration efficiency was compared inside-out and outside-in direct contact membrane distillation (DCMD) modules under the conditions where fouling due to scale formation occurs. The novelty of this work lies in the investigation of the vibration technique to mitigate fouling in both MF and MD processes, which has not been done to the best of our knowledge.

2. Material and methods

2.1. Membrane module

Detailed properties of the MF and MD membrane modules were summarized in Table 1.

2.2. Experimental setup

Experiments were carried out in the bench-scale MF system and the bench-scale DCMD system, which are schematically illustrated in Figs. 1a and b, respectively. Fig. 2 shows the lab-scale vibration system in this study. The vibration system consists of a function generator, an amplifier, and a shaker. The function (signal) generator is a device that can produce various patterns of voltage at a variety of frequencies and amplitudes. The amplifier is an electronic device that can increase the power of a signal. The shaker is a device of laboratory equipment used to vibrate. To deliver constant and regular vibration directly to the module, the following system is constructed.

2.3. Experimental conditions

Table 2 shows experimental conditions of MF and MD system. To examine fouling behaviors of the MF and MD membranes, the feed solution was prepared using NaCl of 35,000 mg/L and $CaSO_4$ of 2,000 mg/L. All reagents were purchased from Sigma Aldrich (St. Louis, MO). The feed pressure was 1 bar in the case of MF. The feed flow and distillate flow rates were 0.9 to 0.6 L/min in the case of MD. The initial feed inlet temperature was 60°C and the distillate inlet temperature ranged was 20°C in the case of MD. The frequency of vibration feed was adjusted from 100 to 200 Hz into both MF and MD.

2.4. Experimental procedures

2.4.1. Fouling tests and calculation of blocking coefficient (b)

To compare fouling propensity in the two operation modes, a series of MF and MD experiments were carried out using the feed water. The effect of flow rate on flux was also examined in the two operation modes. All the tests were done in the batch operation mode. The degree of concentration is expressed as the volume of concentration factor (VCF), which is defined as:

$$\text{VCF} = \frac{V_0}{V_0 - V_p} \quad (1)$$

where V_0 is the initial quantity of feed volume and V_p is the cumulative permeate production. Accordingly, the changes in flux were compared as a function of VCF.

It has been reported that the progress of membrane fouling due to scale formation is caused by the blockage of membrane surface by the deposition of crystals formed from either surface crystallization or bulk crystallization [21,26–29]. Accordingly, the following equations were applied to describe the progress of fouling [30]:

$$J = B(\Delta p)\frac{A_m - A_b}{A_m} = B(\Delta p)(1-\beta) = J_0(1-\beta) \quad (2)$$

Table 1
Properties of MD membrane module

Parameters	MF	MD
Membrane material	PVDF (polyvinylidene fluoride)	PE (polyethylene)
Fiber inside diameter (mm)	0.7	0.57
Fiber outside diameter (mm)	1.15	0.83
Pore size (μm)	0.1	0.1
Porosity (%)	70	70
Membrane area per module (cm^2)	65	65

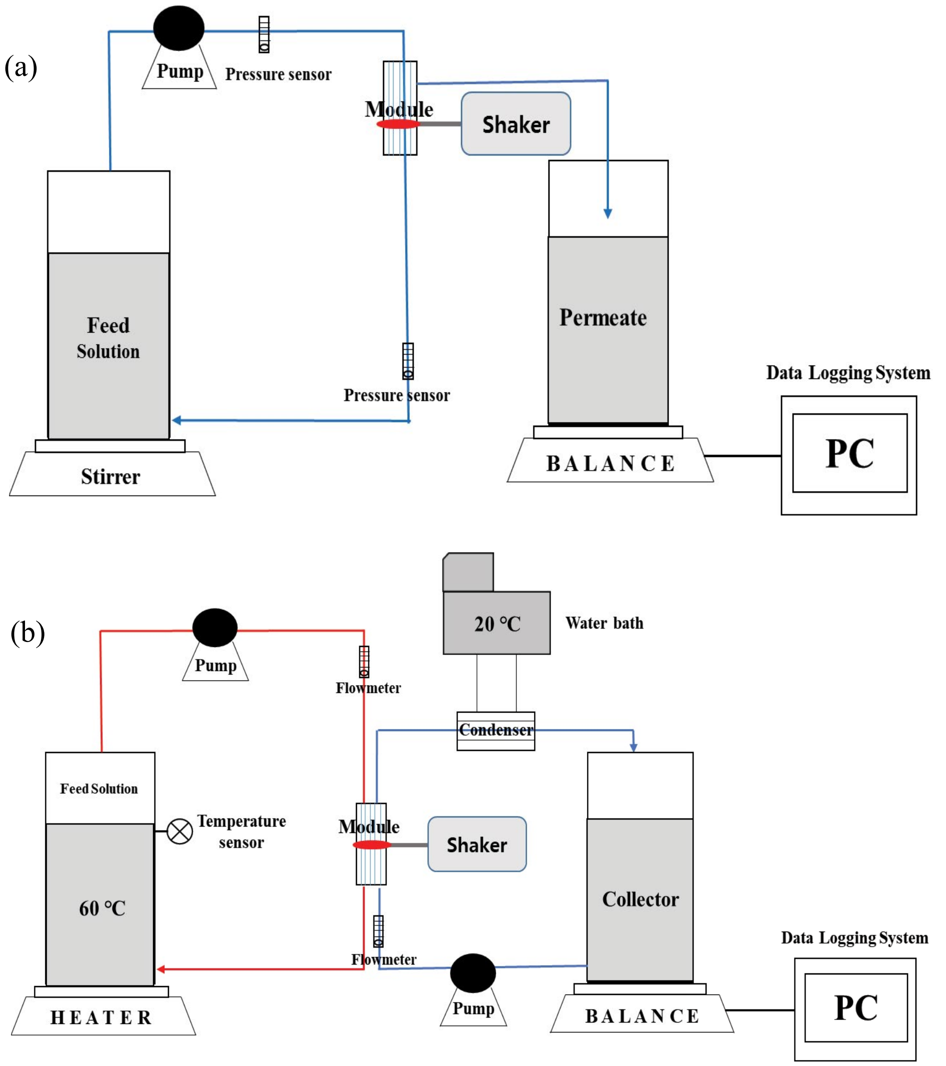

Fig. 1. Schematic diagram of the laboratory (a) MF experimental system and (b) DCMD experimental system.

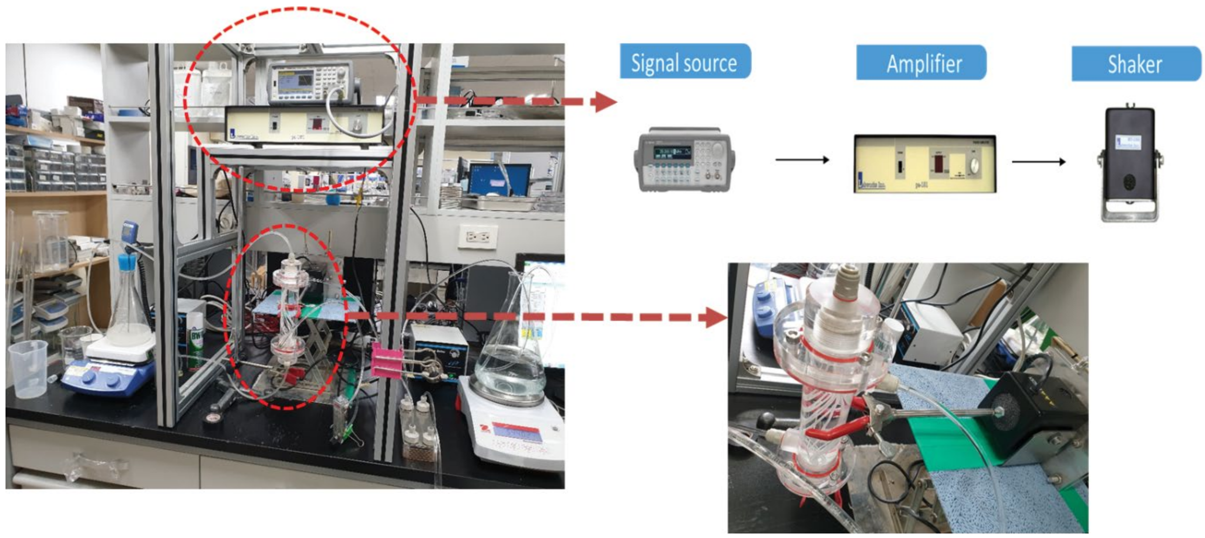

Fig. 2. Lab-scale vibration system.

Table 2
Summary of experimental conditions

Parameters	MF	MD
Raw water	NaCl 35,000 ppm, $CaSO_4$ 2,000 ppm	
Feed flow rate	–	0.9 L/min
Distillate flow rate	–	0.6 L/min
Feed inlet temperature	20°C	60°C
Distillate inlet temperature	20°C	20°C
Operation mode	Outside-in	Inside-out/outside-in
Vibration frequency	100, 200 Hz	
Feed pressure	1 bar	–

where J is the distillate flux, B is the water permeability of MF or MD membrane, A_m is the membrane area, A_b is the membrane area blocked by scales, Δp is the effective difference in the pressure (hydraulic pressure in MF and vapor pressure in MD) between the feed and permeate [31], and β is the blocking coefficient given by A_b/A_m. These equations were developed to describe fouling due to scale formation in membrane systems. They are based on the assumption that the growth of inorganic scales blocks the membrane surface, thereby reducing the effective membrane area [30].

Accordingly, β is calculated using the ratio of flux at a given VCF to the initial flux (J_0):

$$\beta = 1 - \frac{J}{J_0} \quad (3)$$

The physical meaning of β is the ratio of the membrane area which is blocked by the crystals. If β approaches to 1.0, the membrane is completely blocked, implying serious fouling. As VCF increases, the salt concentration increases, leading to an increases rate of crystallization. Therefore, β rapidly increases with VCF during the MF or MD operation.

3. Results and discussion

3.1. Effect of vibration

A series of experiments were performed to compare the fouling propensities by the MF process and the MD process. First, the effect of vibration on the control of MF fouling was examined. Then, the vibration was applied to the MD in two different flow modes including the inside-out and outside-in modes.

3.1.1. Vibration effect on microfiltration

Fig. 3 shows the changes in flux and blocking coefficient on VCF with and without the vibration in the case of the MF process. In Fig. 3a, the flux rapidly decreased in the beginning and the steady-state was reached gradually. Although MF does not reject ions, suspended crystals in the solution resulted in the blockage of the membrane surface, leading to a decrease in flux. The application of the vibration was expected to be effective to retard the membrane fouling by the deposition of the crystal particles. In fact, the vibration at 200 Hz increased the initial flux by more than 10% and also reduced the flux decline, leading to an increase in the final flux.

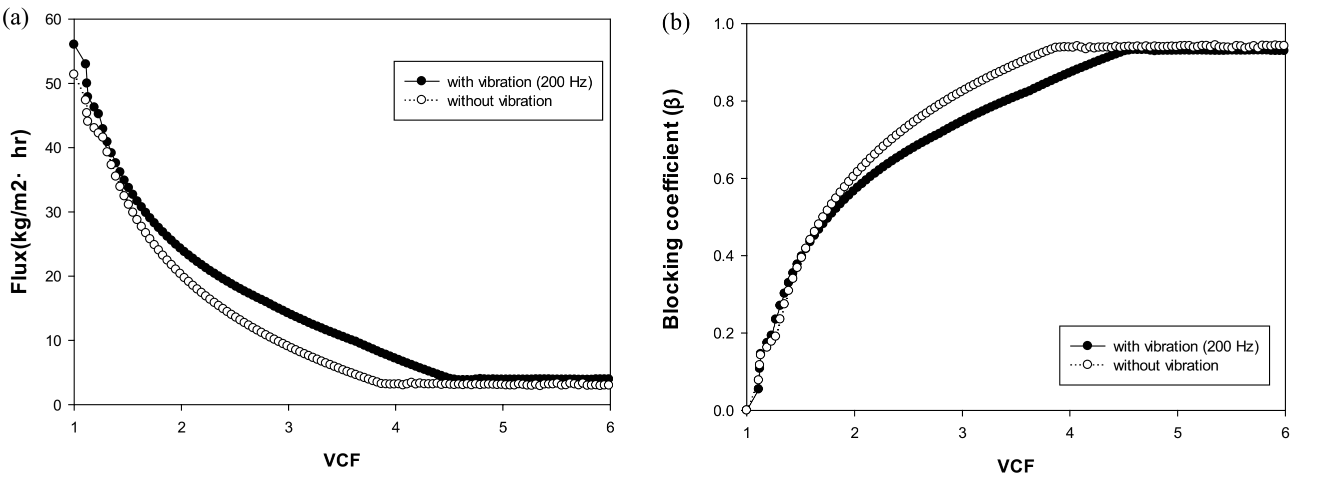

Fig. 3. Dependence of flux and blocking coefficient on VCF during the MF experiments with and without the vibration. (a) Flux and (b) blocking coefficient (symbols: ● with vibration of 200 Hz; ○ without vibration; operating conditions: feed solution: NaCl 35,000 ppm, $CaSO_4$ 2,000 ppm; feed pressure: 1 bar).

To estimate how much membrane surface is blocked by the foulants, the blocking coefficient in Eq. (3) was calculated in each case. As depicted in Fig. 3b, the blocking coefficient also increased in the early stage of the MF operation and reached a steady-state value after the VCF of 3.9. However, the blocking coefficient with the vibration started to increase after the VCF of 4.5. The difference of VCF with or without the vibration was about 0.6 in the MF operation. These results indicate that the MF operation with the vibration is effective to mitigate the fouling.

3.1.2. Vibration effect on membrane distillation

Fig. 4 shows the changes in flux and blocking coefficient on VCF in the MD process. The MD operation was carried out in the inside-out mode, in which the feed is supplied to the lumen side of the fibers and the distillate passes through the shell side of the module. The temperature difference between the feed and the distillate was 40°C (feed temperature: 60°C, distillate temperature: 20°C). The feed flow was 0.9 L/min. As shown in Fig. 4a, the flux without the vibration decreased gradually from the beginning and began to decrease rapidly after VCF of 3.4. The behavior of the flux decline in the MD process was clearly different from the MF process. This is because the fouling mechanisms between the MF and MD processes were different. In MD, the feed solution containing $CaSO_4$ results in the scale formation at high VCF. Accordingly, the fouling becomes severe as the VCF increases.

To mitigate the fouling, the vibration of the module at 200 Hz was applied to the MD process. The results are also shown in Fig. 4a. Compared with the flux decline without

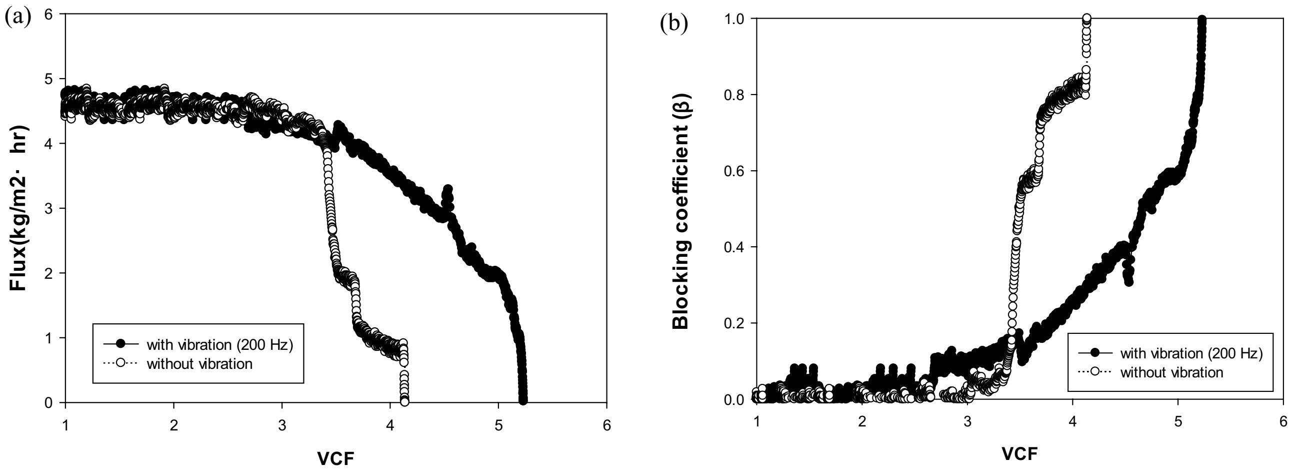

Fig. 4. Dependence of flux and blocking coefficient on VCF during the inside-out DCMD experiments with and without the vibration. (a) Flux and (b) blocking coefficient (symbols: ● with vibration of 200 Hz; ○ without vibration; operating conditions: feed solution: NaCl 35,000 ppm, $CaSO_4$ 2,000 ppm; feed temperature: 60°C; distillate temperature: 20°C; feed flow rate; 0.9 L/min; distillate flow rate; 0.6 L/min).

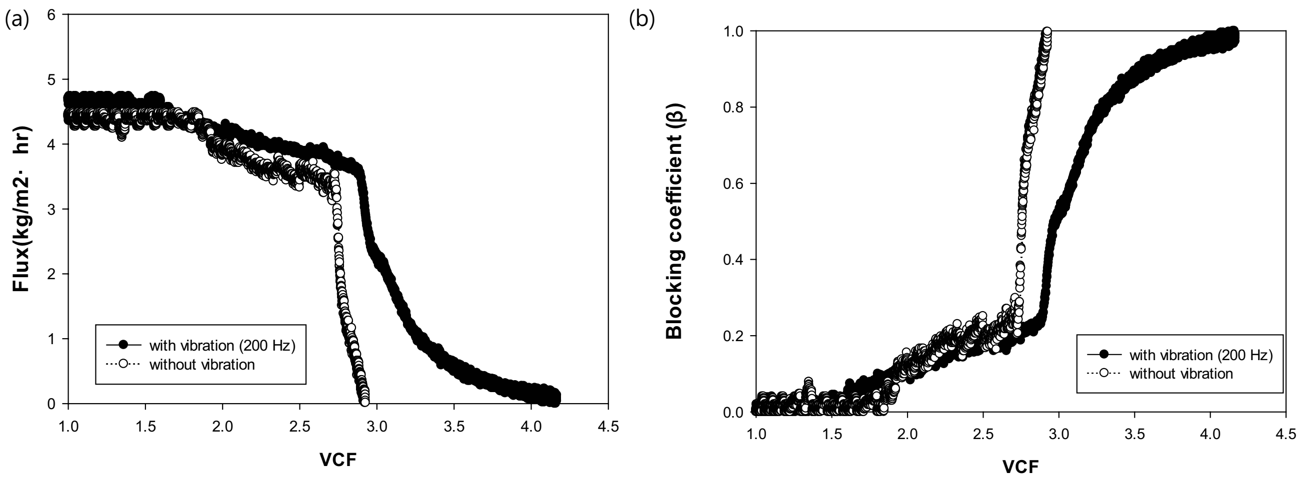

Fig. 5. Dependence of flux and blocking coefficient on VCF during the outside-in DCMD experiments with and without the vibration. (a) Flux and (b) blocking coefficient (symbols: ● with vibration of 200 Hz; ○ without vibration; operating conditions: feed solution: NaCl 35,000 ppm, $CaSO_4$ 2,000 ppm; feed temperature: 60°C; distillate temperature: 20°C; feed flow rate; 0.9 L/min; distillate flow rate; 0.6 L/min).

the vibration, it was significantly retarded. The effect of the vibration on the fouling control was higher in MD than in MF. This suggests that the vibration can be a promising technique for fouling control in MD processes that have potential problems associated with scale formation.

The blocking coefficients were also compared for the MD processes without and with the vibration. As depicted in Fig. 4b, a rapid increase in the blocking coefficient was observed at the VCF of 3.4 without the vibration. The membrane seems to be completed blocked at the VCF of 4.1 without the vibration. However, the increase in the blocking coefficient was less significant with the vibration. In this case, the complete blocking of the membrane was found at the VCF of 5.2. It is evident from these results that the vibration is effect to retard the blockage of the membrane due to scale formation.

3.1.3. Comparison of outside-in MD with the inside-out MD

Experiments were carried out with the MD process in the outside-in mode, in which the feed is supplied to the shell side of the module and the distillate passes through the lumen side of the fibers. All the other conditions were maintained constant to examine the effect of flow mode on the vibration effect. Fig. 5a shows the flux behaviors with VCF, which was similar to the case with the inside-out-mode. Nevertheless, the effect of vibration on fouling control was slightly different. Although the vibration was effect to retard the flux decline in the outside-in mode, it was less efficient than that in the inside-out mode. This suggests that the vibration is more suitable for the inside-out mode MD than the outside-out mode MD.

The blocking coefficients were also compared in the outside-in MD without and with the vibration. The results are summarized in Fig. 5b. When the VCF was 2.9, the blocking coefficients was almost 1 in the operation without the vibration, indicating that the membrane was completely blocked by the foulant. With the vibration, the VCF was 4.1 and the membrane was completely blocked. It was also confirmed that the vibration is less effective to control fouling in the outside-in mode than in the inside-out mode.

The proposed mechanism of the antifouling effect by the vibration is schematically illustrated in Fig. 6. The vibration can prevent the formation of crystal particles in the solution phase. Moreover, an increased shear rate by the vibration can prevent the deposition of the crystal particles. In MF, the deposition of the particulate foulants is reduced by the vibration but both crystal formation and deposition can be retarded by the vibration in MD. Accordingly, the antifouling effect by the vibration can be higher in MD than in MF.

To further investigate the antifouling mechanisms by the vibration, the MD modules were visually examined after the experiments to compare the differences between the two modes after the fouling. In the inside-out mode, there were substantial amounts of scales attaching to the inlet channel of the module as depicted in Fig. 7a. However, in the outside-in mode, a large amount of scales was found on the surface of the fibers as demonstrated in Fig. 7b. The scale formation in the inside-out mode mainly occurs near the inlet section of the fibers. During the DCMD operation, scales are generated through the bulk crystallization and enter in the fibers, thereby clogging the fibers. Although the remaining part of the fiber may be clean without scale deposits, it may not be used for water production because the feed water cannot enter. A relatively small amount

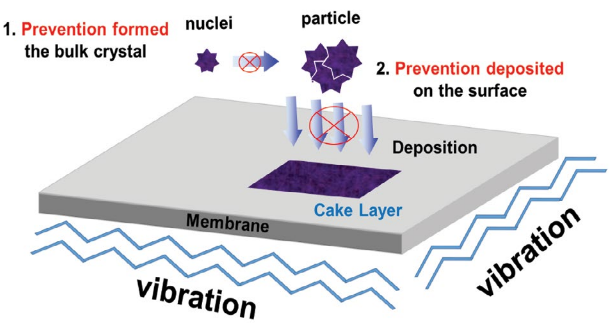

Fig. 6. Vibration effect for mitigating fouling.

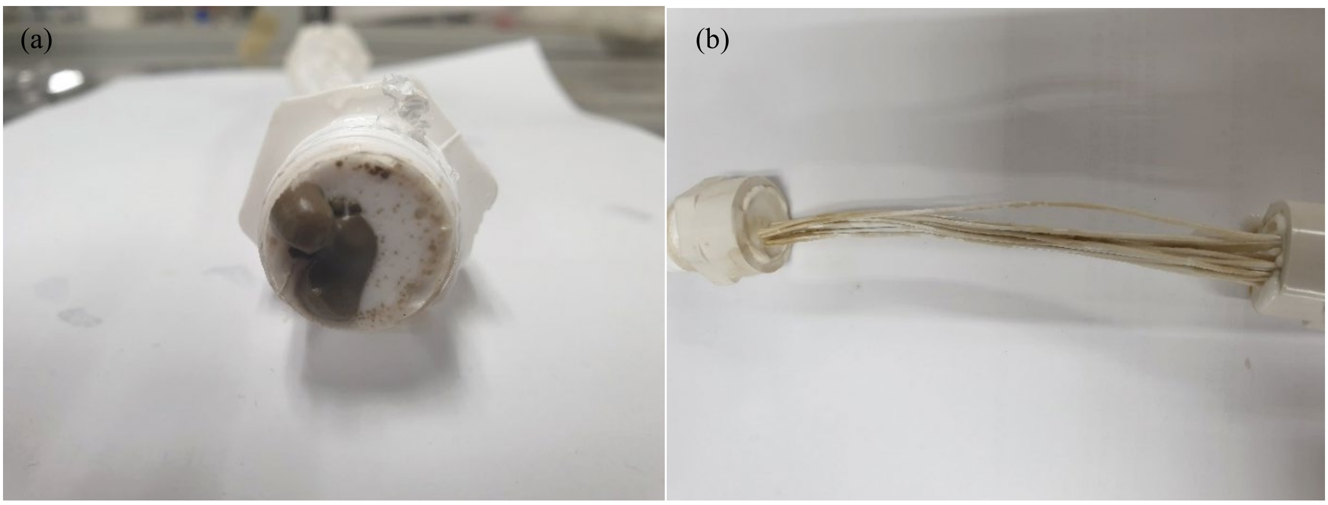

Fig. 7. Photographs of the membrane module after DCMD experiments. (a) Inside-out mode and (b) outside-in mode.

of crystals can block the fibers and thus the flux decline due to scale formation rapidly occurs. On the other hand, the scale formation in the outside-in mode occurs on the outer surface of the fibers.

Since the vibration can detach the foulants from the membrane and modules, the scales on the inlet part of the module can be readily removed by the application of the vibration. But the removal of scales on the fiber surfaces is rather difficult by the vibration. When the membrane is being vibrated, the fibers can move due to their flexibility. Accordingly, the energy by the vibration is inefficiently transferred and lost due to the fiber movement, which is the case with the outside-in MD. If the inlet part is fixed, which is the case with the inside-out MD, the vibrational energy can be directly transferred. This is why the vibration is more effective in the inside-out MD than the inside-out MD.

3.2. Effect of the vibration frequency

Vibration frequency is an important factor affecting the antifouling effect by the vibration. Accordingly, the effect of the frequency was investigated in the two operation modes. Two frequencies were compared, including 100 and 200 Hz. In Fig. 8, the flux and blocking coefficient in the inside-out MD are shown as a function of VCF at the two frequencies. The initial fluxes of 200 Hz were higher and flux declines were also less serious than 100 Hz. The blocking coefficients of 200 Hz gradually increased to more than 100 Hz. Similar results were observed in the outside-in MD mode as presented in Fig. 9. As the vibration frequency increases from 100 to 200 Hz, the flux increased and the blocking coefficient was reduced. However, the difference between the two frequencies was not very much significant.

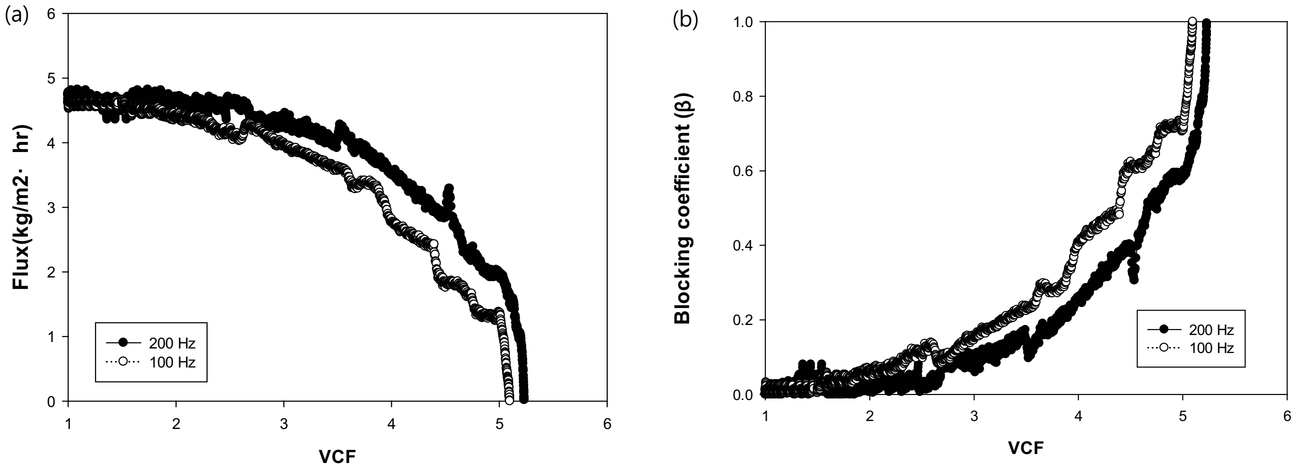

Fig. 8. Dependence of flux and blocking coefficient on VCF during the insdie-out DCMD experiments with and without the vibration. (a) Flux and (b) blocking coefficient (symbols: ● with vibration of 200 Hz; ○ with vibration of 100 Hz; operating conditions: feed solution: NaCl 35,000 ppm, $CaSO_4$ 2,000 ppm; feed temperature: 60°C; distillate temperature: 20°C; feed flow rate; 0.9 L/min; distillate flow rate; 0.6 L/min).

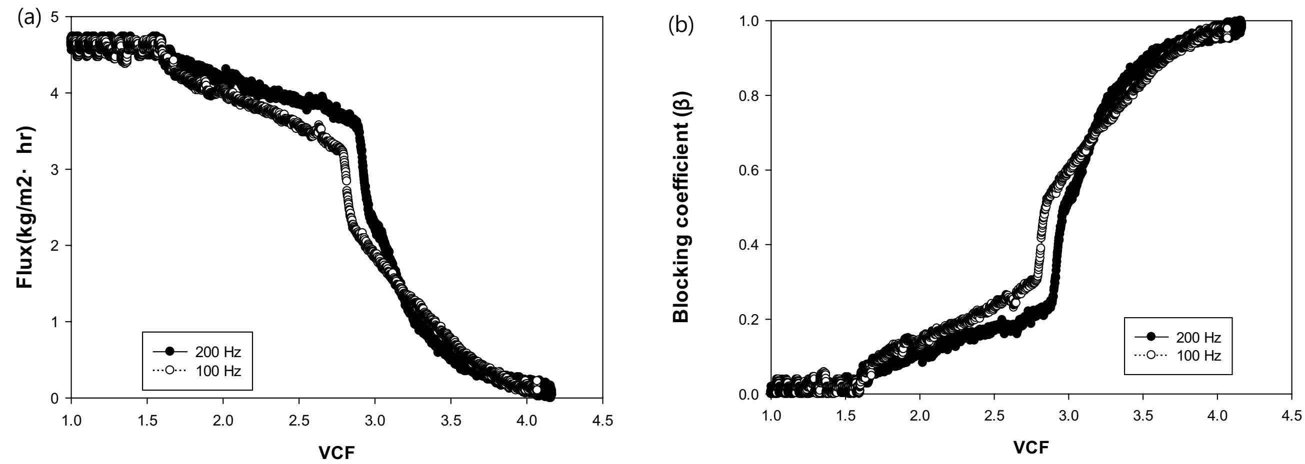

Fig. 9. Dependence of flux and blocking coefficient on VCF during the outsdie-in DCMD experiments with and without the vibration. (a) Flux and (b) blocking coefficient (symbols: ● with vibration of 200 Hz; ○ with vibration of 100 Hz; operating conditions: feed solution: NaCl 35,000 ppm, $CaSO_4$ 2,000 ppm; feed temperature: 60°C; distillate temperature: 20°C; feed flow rate; 0.9 L/min; distillate flow rate; 0.6 L/min).

4. Conclusions

This study examined the effect of vibration on fouling propensity of hollow fiber membranes in MF and MD processes. The following conclusions were withdrawn:

- In both MF and MD processes, the vibration was found to be effective to migrated fouling by the solution containing scale-forming ions. The fouling in MF was caused by the deposition of crystal particles and that in MD resulted from the crystal formation. Due to the difference in the fouling mechanisms, the vibration was more effective to control fouling in MD than in MF.
- The blocking coefficients were estimated from the experimental results on flux decline. A significant retardation of the membrane blockage was observed by the application of the vibration.
- The vibration works more efficiently in the inside-out MD than in the outside-in MD. This is attributed to the different efficiency of the energy transfer by the vibration. When the inlet part of the module was blocked, which is the case with the inside-out MD, the vibration was effective due to negligible loss of vibrational energy. When the surfaces of the membrane fiber were blocked, which is the case with the outside-in MD, the vibration effect was smaller due to the energy loss by the fiber movement.
- As an increase in the vibration frequency, the antifouling effect increased in both the inside-out and the outside-in mode MD processes.

Acknowledgment

This subject is supported by Korea Ministry of Environment as "Global Top Project (2017002100001)" and this study was funded by the Korea Ministry of Environment (MOE) and Korea Environmental Industry and Technology Institute (KEITI) as "A Industrial Facilities and Infrastructure Research Program" (1485016250).

References

[1] M. Mulder, Basic Principles of Membrane Technology, 2nd ed., Kluwer Academic, Dordrecht, Boston, MA, 1996.
[2] M.Y. Jaffrin, Dynamic shear-enhanced membrane filtration: a review of rotating disks, rotating membranes and vibrating systems, J. Membr. Sci., 324 (2008) 7–25.
[3] F. Wicaksana, A.G. Fane, V. Chen, Fibre movement induced by bubbling using submerged hollow fibre membranes, J. Membr. Sci., 271 (2006) 186–195.
[4] S.R. Bellara, Z.F. Cui, D.S. Pepper, Gas sparging to enhance permeate flux in ultrafiltration using hollow fibre membranes, J. Membr. Sci., 121 (1996) 175–184.
[5] Z.F. Cui, S. Chang, A.G. Fane, The use of gas bubbling to enhance membrane processes, J. Membr. Sci., 221 (2003) 1–35.
[6] L.J. Xia, A.W.K. Law, A.G. Fane, Hydrodynamic effects of air sparging on hollow fiber membranes in a bubble column reactor, Water Res., 47 (2013) 3762–3772.
[7] T. Li, A.W.K. Law, M. Cetin, A.G. Fane, Fouling control of submerged hollow fibre membranes by vibrations, J. Membr. Sci., 427 (2013) 230–239.
[8] R. Bouzerar, L.H. Ding, M.Y. Jaffrin, Local permeate flux-sheer-pressure relationships in a rotating disk microfiltration module: implications for global performance, J. Membr. Sci., 170 (2000) 127–141.
[9] L.F. Liu, B. Gao, J.D. Liu, F.L. Yang, Rotating a helical membrane for turbulence enhancement and fouling reduction, Chem. Eng. J., 181 (2012) 486–493.
[10] O. Al Akoum, M.Y. Jaffrin, L.H. Ding, P. Paullier, C. Vanhoutte, An hydrodynamic investigation of microfiltration and ultrafiltration in a vibrating membrane module, J. Membr. Sci., 197 (2002) 37–52.
[11] S.C. Low, H.H. Juan, L.K. Siong, A combined VSEP and membrane bioreactor system, Desalination, 183 (2005) 353–362.
[12] G. Amy, N. Ghaffour, Z.Y. Li, L. Francis, R.V. Linares, T. Missimer, S. Lattemann, Membrane-based seawater desalination: present and future prospects, Desalination, 401 (2017) 16–21.
[13] D.L. Zhao, S.C. Chen, C.X. Guo, Q.P. Zhao, X.M. Lu, Multifunctional forward osmosis draw solutes for seawater desalination, Chin. J. Chem. Eng., 24 (2016) 23–30.
[14] N. Ghaffour, J. Bundschuh, H. Mahmoudi, M.F.A. Goosen, Renewable energy-driven desalination technologies: a comprehensive review on challenges and potential applications of integrated systems, Desalination, 356 (2015) 94–114.
[15] A. Subramani, J.G. Jacangelo, Emerging desalination technologies for water treatment: a critical review, Water Res., 75 (2015) 164–187.
[16] A. Alkhudhiri, N. Darwish, N. Hilal, Membrane distillation: a comprehensive review, Desalination, 287 (2012) 2–18.
[17] E. Drioli, A. Ali, F. Macedonio, Membrane distillation: recent developments and perspectives, Desalination, 356 (2015) 56–84.
[18] I. Hitsov, T. Maere, K. De Sitter, C. Dotremont, I. Nopens, Modelling approaches in membrane distillation: a critical review, Sep. Purif. Technol., 142 (2015) 48–64.
[19] M.A. Abu-Zeid, Y.Q. Zhang, H. Dong, L. Zhang, H.L. Chen, L. Hou, A comprehensive review of vacuum membrane distillation technique, Desalination, 356 (2015) 1–14.
[20] B.B. Ashoor, S. Mansour, A. Giwa, V. Dufour, S.W. Hasan, Principles and applications of direct contact membrane distillation (DCMD): a comprehensive review, Desalination, 398 (2016) 222–246.
[21] L. Fortunato, Y.S. Jang, J.G. Lee, S. Jeong, S. Lee, T. Leiknes, N. Ghaffour, Fouling development in direct contact membrane distillation: non-invasive monitoring and destructive analysis, Water Res., 132 (2018) 34–41.
[22] Y. Choi, G. Naidu, S. Jeong, S. Vigneswaran, S. Lee, R. Wang, A.G. Fane, Experimental comparison of submerged membrane distillation configurations for concentrated brine treatment, Desalination, 420 (2017) 54–62.
[23] Y. Li, C.L. Jin, Y.L. Peng, Q.F. An, Z.P. Chen, J.C. Zhang, L. Ge, S.B. Wang, Fabrication of PVDF hollow fiber membranes via integrated phase separation for membrane distillation, J. Taiwan Inst. Chem. Eng., 95 (2019) 487–494.
[24] L. Cheng, Y.J. Zhao, P.L. Li, W.L. Li, F. Wang, Comparative study of air gap and permeate gap membrane distillation using internal heat recovery hollow fiber membrane module, Desalination, 426 (2018) 42–49.
[25] H. Cho, Y. Choi, S. Lee, Effect of pretreatment and operating conditions on the performance of membrane distillation for the treatment of shale gas wastewater, Desalination, 437 (2018) 195–209.
[26] H.J. Oh, Y.K. Choung, S. Lee, J.S. Choi, T.M. Hwang, J.H. Kim, Scale formation in reverse osmosis desalination: model development, Desalination, 238 (2009) 333–346.
[27] S. Lee, J. Kim, C.H. Lee, Analysis of $CaSO_4$ scale formation mechanism in various nanofiltration modules, J. Membr. Sci., 163 (1999) 63–74.
[28] S. Lee, C.H. Lee, Effect of operating conditions on $CaSO_4$ scale formation mechanism in nanofiltration for water softening, Water Res., 34 (2000) 3854–3866.
[29] J.G. Lee, Y. Jang, L. Fortunato, S. Jeong, S. Lee, T. Leiknes, N. Ghaffour, An advanced online monitoring approach to study the scaling behavior in direct contact membrane distillation, J. Membr. Sci., 546 (2018) 50–60.
[30] L.D. Tijing, Y.C. Woo, J.S. Choi, S. Lee, S.H. Kim, H.K. Shon, Fouling and its control in membrane distillation–a review, J. Membr. Sci., 475 (2015) 215–244.
[31] M.H. Sharqawy, J.H. Lienhard, S.M. Zubair, Thermophysical properties of seawater: a review of existing correlations and data, Desal. Water Treat., 16 (2010) 354–380.